Current Optics and Photonics
Vol. 4, No. 6, December 2020, pp. 461-465

ISSN: 2508-7266(Print) / ISSN: 2508-7274(Online)
DOI: https://doi.org/10.3807/COPP.2020.4.6.461

In-line Dual-Mode DBR Laser Diode for Terahertz Wave Source

Youngchul Chung*

Department of Electronics and Communication Engineering, Kwangwoon University, Seoul 01897, Korea

(Received August 20, 2020 : revised October 23, 2020 : accepted October 26, 2020)

A dual-mode laser terahertz source consisting of two in-line distributed Bragg reflector (DBR) laser diodes (LD) is proposed. It is less susceptible to residual reflections from facets than an in-line dual-mode distributed feedback (DFB) LD. The characteristics of the proposed terahertz source are theoretically investigated using a split-step time-domain simulation. It is shown that terahertz waves of frequencies from 385 GHz to 1725 GHz can be generated by appropriate thermal tuning of two DBR LDs. The dual-mode DBR LD terahertz source exhibits good spectral quality for residual facet reflectivity below 0.02, but facet reflectivity of the in-line dual-mode DFB LD terahertz source should be below 0.002 to provide similar spectral quality.

Keywords : Dual-Mode laser, Terahertz wave, Distributed-Bragg-Reflector laser diode, Time-Domain modeling
OCIS codes : (000.4430) Numerical approximation and analysis; (110.6795) Terahertz imaging; (140.3490) Lasers, distributed-feedback; (250.5960) Semiconductor lasers

I. INTRODUCTION

Terahertz wave science and technology have been developed over the last 30 years. In the 1980s and 1990s, terahertz waves were used primarily in astronomy and spectroscopy. After the development of terahertz time-domain spectroscopy based on lasers in the 1980s and 1990s, the terahertz wave has been rapidly employed for many disciplines. For example, terahertz waves can be utilized as a novel tool for evaluating solar cells employing a laser terahertz emission microscope (LTEM) [1], or they could be used for the realization of next-generation airport inspection systems due to the transparency of most non-conductive materials in the terahertz frequencies [2]. In addition, the terahertz wave in 0.1-0.3 THz frequency band provides potentially enormous bandwidth for next-generation 6G wireless communication networks [3].

A continuous wave (CW) terahertz wave can be generated through photo-mixing in a dual-mode optical source. A variety of dual-mode optical sources whose mode spacing can be tuned up to ~1 THz without mode hopping have been reported [4-6]. Monolithically integrated dual-mode laser sources with two parallel cavity structures have been reported [6-8]. Even though this kind of terahertz laser source provides a wide tuning range, an in-line dual-mode laser tends to provide better spectral quality of CW terahertz wave than the parallel-cavity source.

Monolithically integrated in-line dual-mode laser diodes consisting of two in-line distributed feedback (DFB) laser diodes (LDs) have been reported [9-11]. The dual-mode laser diodes consisting of two in-line DFB LDs exhibited a tuning range of 0.38-1.12 THz which was used for the demonstration of a compact THz spectroscopy system [11]. In this paper, a dual-mode laser diode consisting of two in-line distributed Bragg reflector (DBR) LDs is proposed. The proposed dual-mode DBR LD has a potential to be less dependent on the residual reflections from the facets because two DBR LDs are quite independent from each other due to the detuned Bragg reflectors and the residual facet reflections are mostly prohibited from being introduced to the DBR LD cavities due to the leftmost and rightmost Bragg reflectors. The lasing characteristics of the in-line dual-mode DBR LD are theoretically studied with a split-step time-domain modeling and compared with those of the in-line dual-mode DFB LD.

*Corresponding author: ychung@kw.ac.kr, ORCID 0000-0002-2460-2618
Color versions of one or more of the figures in this paper are available online.

II. DEVICE STRUCTURE

The proposed in-line dual-mode DBR LD is illustrated in Fig. 1, in which two DFB LDs of the in-line dual-mode DFB LD [9-11] are replaced by two DBR LDs. A phase section is placed between two DBR LDs for the suppression of the facet-to-facet cavity modes [11]. The losses of the facet-to-facet cavity modes can be increased by the reverse bias onto the phase section, which aids the independent lasing of two DBR LDs. The wavelength of each DBR LD can be adjusted by the heating currents through the tuning pads on the DBRs. The proposed dual-mode DBR LD has a potential to be less dependent on the residual reflections from the facets because two DBR LD's are quite independent from each other due to the detuned Bragg reflectors and the residual reflections from the facets are mostly prohibited from being introduced to the DBR LD cavities due to the leftmost and rightmost Bragg reflectors.

In Fig. 1, the lengths of the semiconductor optical amplifier (SOA), LD active sections, DBRs, phase sections of the left and right DBR LD, and the center phase section in the overall in-line dual-mode DBR LD are 500, 200, 50, 40, and 50 μm, respectively. The length of the whole device is 1230 μm which is a little bit larger than half the length of the widely tunable SOA-integrated DBR laser by combination of sampled and superstructure gratings [12] and the proposed device is believed to be well realized using the state-of-the-art InP photonic integrated circuit fabrication process [13].

III. SIMULATION RESULTS

The performance of the proposed in-line dual-mode DBR LD is theoretically investigated using the split-step time-domain modeling which is described in [14, 15]. In the simulation, the whole structure is sliced into small sections. The time step in the modeling should be the propagation time of the optical wave through a sliced small section [14, 15]. In each small section the gain and phase operations are performed followed by the backward coupling operation due to the grating wherever it exists to trace the evolution of optical waves during a time step. Assume that the left DBR-LD lases near 1548.3 nm and the right one lases near 1534.5 nm with no heating currents into the tuning pads. In the simulation, the spontaneous and Auger carrier

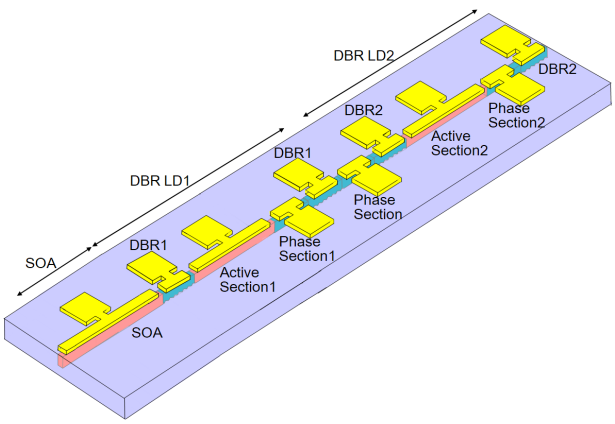

FIG. 1. Configuration of in-line dual-mode DBR LD.

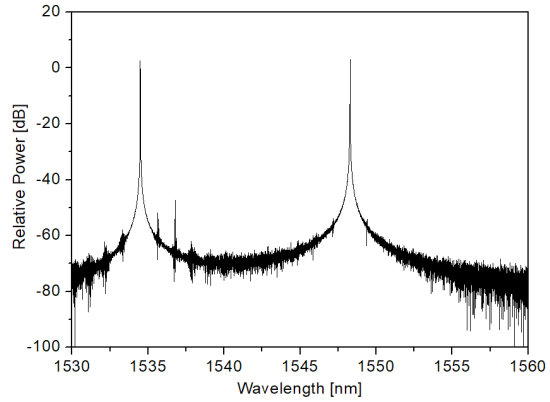

(a)

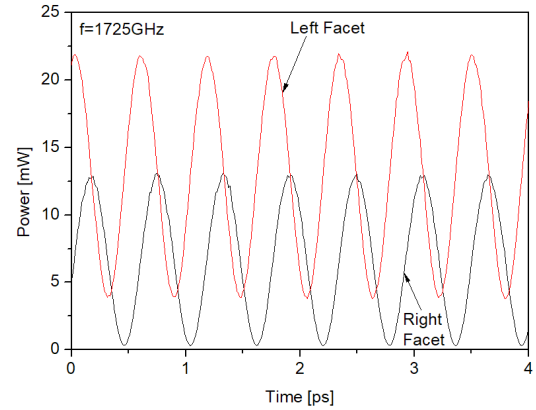

(b)

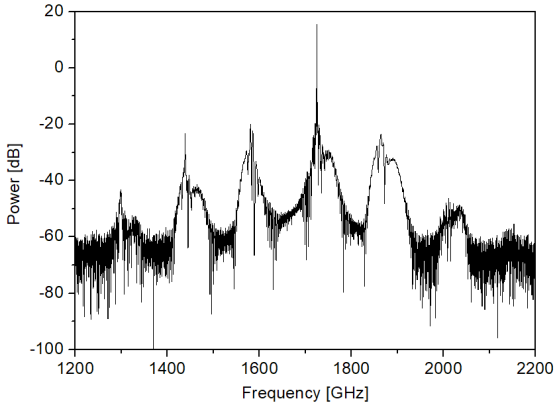

(c)

FIG. 2. Simulation results of the in-line dual-mode DBR LD in case of 300 cm^{-1} loss in the phase section, which show (a) the optical spectrum exhibiting the dual mode lasing at the wavelength of 1534.3 nm and 1548.3 nm, (b) the time-domain terahertz waveform at 1725 GHz due to the beating of two optical modes, and (c) the terahertz wave spectrum.

recombination coefficients are 1.0×10^{-10} cm^3s^{-1} and 1.3×10^{-28} cm^6s^{-1}, respectively. The carrier life time is 10 ns. The transparency carrier density and the differential gain are 1.5×10^{18} cm^3 and 4.0×10^{-16} cm^2, respectively. The line-width enhancement factor is 3, the waveguide loss in the lasing section is 30 cm^{-1} and the effective group refractive index 3.7. The waveguide confinement factor in LD and SOA active waveguide region is 0.17 and that in the passive waveguide region for phase or loss tuning is 0.51. The waveguide width and the active layer thickness are 1.5 μm and 0.12 μm, respectively. The coupling coefficient of the Bragg grating is 150 cm^{-1}, which corresponds to $\kappa L_g = 0.75$.

The absorption loss by the reverse bias to the phase region between two DBR LDs is required to suppress the lasing of the facet-to-facet cavity mode. When the absorption coefficient through the phase section is 300 cm^{-1} which results in the loss of 6.5 dB over the 50 μm-long center phase region, the facet-to-facet cavity mode is observed to be almost completely suppressed. When the current into the active regions of the left DBR-LD is 70 mA and that into the right DBR-LD 150 mA, the lasing power from two DBR-LDs are balanced. The output power is measured at the left facet. With the above injection currents into active regions and the current into SOA being 120 mA, the simulation result for the optical spectrum from the dual-mode DBR LD is shown in Fig. 2(a). The mixing of two optical waves at the wavelength of 1548.3 nm and 1534.3 nm results in the terahertz wave at the frequency of 1725 GHz as shown in Fig. 2(b), whose spectrum is shown in Fig. 2(c). As shown in Fig. 2(b), the average power from the left facet is about 17 mW (12.3 dBm) which might be low considering the packaging loss. The output power can be increased by properly adjusting the laser injection currents and the SOA current. The experimental results for the device with similar structures such as the sampled or superstructure grating tunable laser diode integrated with a SOA show that the output power can be as large as 45 mW (16 dBm) [12]. The tuning characteristics of the terahertz source are investigated and shown in Figs. 3(a) and 3(b). As the right tuning pad is heated so that the refractive index of DBR2 is increased by 0.05, the lasing wavelength of the right DBR-LD is changed from 1534.5 nm to 1545.2 nm while that of the left DBR-LD is maintained to be near 1548.3 nm as shown in Fig. 3. As a result, the terahertz wave frequency can be tuned from 1725 GHz to 385 GHz, which is shown in Fig. 3(b).

In the above discussions, the facet reflectivity values of the device are assumed to be zero. For the increasing facet reflectivity values the dual-mode lasing characteristics are calculated and the optical spectra are shown in Fig. 4(a). In this simulation, the tuning pads are properly heated so that 1725 GHz wave is generated. Figure 4(a) shows that the facet power reflectivity as large as 0.36 does not seem to deteriorate the performance of the dual-mode lasing characteristics. The terahertz power spectrum variation

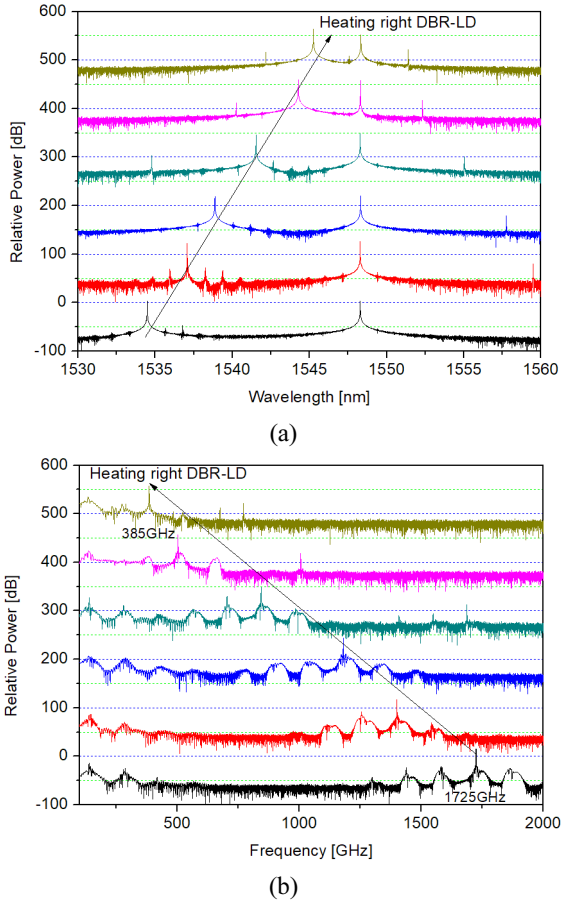

FIG. 3. Tuning characteristics of the in-line dual-mode DBR LD. (a) the lasing wavelength of the right DBR-LD is tuned from 1534.5 nm to 1545.2 nm as the right tuning pad is heated so that the refractive index of the right DBRs is increased by 0.05. (b) variation of terahertz wave spectrum as the right micro-heater is heated so that the refractive index of the right DBRs is increased by 0.05. With this tuning, the terahertz wave frequency is tuned from 1725 GHz to 385 GHz.

versus the facet power reflectivity increase is calculated and shown in Fig. 4(b). The observation of the power spectra indicates that the facet reflectivity larger than 0.02 introduces side frequency components 20 GHz apart from the main frequency component. The enlarged spectra for the facet reflectivity of 0.003, 0.005, 0.01, and 0.02 are shown in Fig. 4(c) and the detailed THz spectrum for the facet reflectivity of 0.02 is shown in Fig. 4(d). From Figs. 4(c) and 4(d) it is observed that the full spectral width at -10 dB is maintained to be about 30 MHz as the facet reflectivity increases up to 0.02. The actual spectral width could be lower because the frequency resolution of the fast Fourier transform (FFT) calculation is about 10 MHz in this simulation.

For the comparison of performance deterioration due to the imperfection of anti-reflection coating, the characteristics of the in-line dual-mode DFB LD which was discussed in the previous report [13] are investigated. The in-line DFB

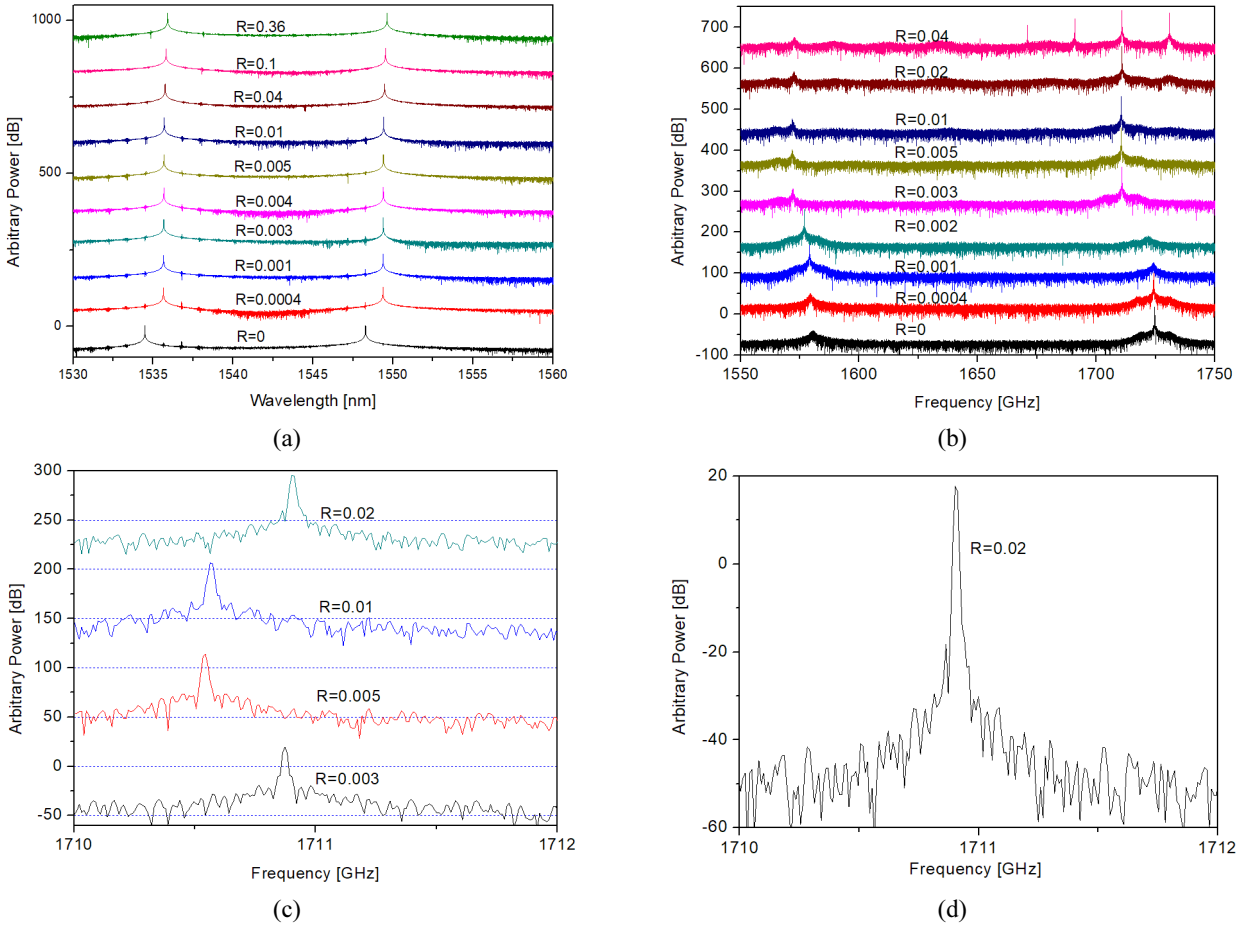

FIG. 4. Effects of facet reflection on the dual-mode DBR LD characteristics. (a) optical wave spectra and (b) terahertz wave spectra of the dual-mode DBR LD for various facet reflectivity values, (c) enlarged spectra for the facet reflectivity of from 0.003 to 0.02, and (d) detailed terahertz spectrum for the facet reflectivity of 0.02.

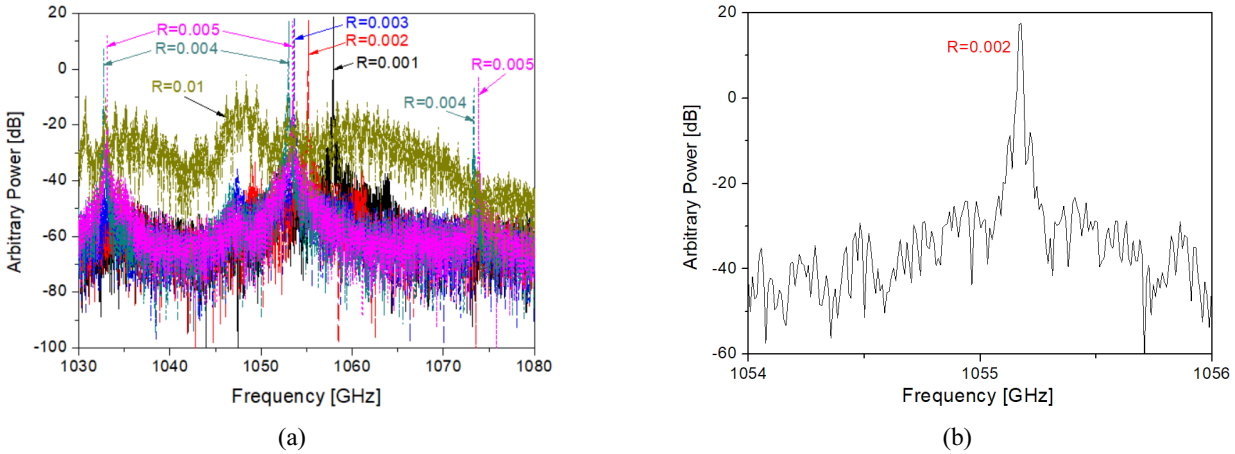

FIG. 5. Effects of facet reflection on the dual-mode DFB LD characteristics. (a) Terahertz output power spectrum variation of the dual-mode DFB LD versus the facet power reflection increase and (b) detailed spectrum for the facet reflectivity of 0.002.

LDs are 700 μm-long. The phase section and SOA are 50 μm and 700 μm-long, respectively. When the injection currents into two DFB-LDs are 70 mA, the lasing wavelengths from two DFB-LDs are 1308.3 nm and 1304.2 nm, and the terahertz wave of 1057.8 GHz is generated. The current into the SOA is 150 mA. The terahertz power spectrum variation versus the facet power reflectivity increase is investigated and shown in Fig. 5(a). The observation of

the power spectra indicates that the facet reflectivity larger than 0.002 introduces side frequency components 20 GHz apart from the main frequency component. The enlarged spectrum for the facet reflectivity of 0.002 is shown in Fig. 5(b) and the full spectral width at -10 dB is observed to be about 30 MHz. The facet power reflectivity should be lower than 0.002 for good spectral quality in the terahertz wave generation. The facet reflectivity of the dual-mode DFB LD should be maintained to be 10 times lower than that of the dual-mode DBR LD.

IV. CONCLUSIONS

An in-line dual-mode laser terahertz source consisting of two DBR LDs is theoretically studied using a split-step time-domain modeling. In the calculations, the device is sliced into a number of small sections. In each small section, the gain and phase operations are performed and the backward coupling operation caused by the grating wherever it exists is stably incorporated. This operation is repeated to trace the evolution of optical wave in the device. It is shown that the terahertz wave generation from 385 GHz to 1725 GHz could be achieved through the proper combination of thermal tuning of two DBR LDs. The residual facet reflectivity to guarantee good spectral quality should be lower than 0.02 for the in-line dual-mode DBR LD while that should be lower than 0.002 for the in-line dual-mode DFB LD.

ACKNOWLEDGMENT

This work was supported by the Research Grant of Kwangwoon University in 2019.

REFERENCES

1. H. Nakanishi, S. Fujiwara, K. Takayama, I. Kawayama, H. Murakami, and M. Tonouchi, "Imaging of a polycrystalline silicon solar cell using a laser terahertz emission microscope," Appl. Phys. Express **5**, 112301 (2012).
2. L. Ho, M. Pepper, and P. Taday, "Signatures and fingerprints," Nat. Photon. **2**, 541-543 (2008).
3. L. Yan, C. Han, and J. Yuan. "Hybrid precoding for 6G terahertz communications: performance evaluation and open problems," in *Proc. 2nd 6G Wireless Summit - 6G SUMMIT* (Levi, Finland, Mar. 2020), pp. 1-5.
4. P. J. Moore, Z. J. Chaboyer, and G. Das, "Tunable dual-wavelength fiber laser," Opt. Fiber Technol. **15**, 377-379 (2009).
5. M. Y. Jeon, N. Kim, J. Shin, J. S. Jeong, and S.-P. Han, C. W. Lee, Y. A. Leem, D.-S. Yee, H. S. Chun, and K. H. Park, "Widely tunable dual-wavelength Er^{3+}-doped fiber laser for tunable continuous-wave terahertz radiation," Opt. Express **18**, 12291-12297 (2010).
6. B. Sartorius, M. Schlak, D. Stanze, H. Roehle, H. Künzel, D. Schmidt, H.-G. Bach, R. Kunkel, and M. Schell, "Continuous wave terahertz systems exploiting 1.5 μm telecom technologies," Opt. Express **17**, 15001-15007 (2009).
7. M. Theurer, T. Göbel, D. Stanze, U. Troppenz, F. Soares, N. Grote, and M. Schell, "Photonic-integrated circuit for continuous-wave THz generation," Opt. Lett. **38**, 3724-3726 (2013).
8. A. J. Seeds, M. J. Fice, K. Balakier, M. Natrella, O. Mitrofanov, M. Lamponi, M. Chtioui, F. van Dijk, M. Pepper, G. Aeppli, A. G. Davies, P. Dean, E. Linfield, and C. C. Renaud, "Coherent terahertz photonics," Opt. Express **21**, 22988-23000 (2013).
9. N. Kim, Y. A. Leem, H. Ko, M. Y. Jeon, C. W. Lee, S.-P. Han, D. Lee, and K. H. Park, "Widely tunable 1.55-μm detuned dual-mode laser diode for compact continuous-wave THz emitter," ETRI J. **33**, 810-813 (2011).
10. N. Kim, H.-C. Ryu, D. Lee, S.-P. Han, H. Ko, K. Moon, J.-W. Park, M. Y. Jeon, and K. H. Park, "Monolithically integrated optical beat sources toward a single-chip broadband terahertz emitter," Laser Phys. Lett. **10**, 085805 (2013).
11. E. S. Lee, N. Kim, S.-P. Han, D. Lee, W.-H. Lee, K. Moon, I.-M. Lee, J.-H. Shin, and K. H. Park, "SOA-integrated dual-mode laser and PIN-photodiode for compact CW terahertz system," ETRI J. **38**, 665-674 (2016).
12. M. Gotoda, T. Nishimura, and Y. Tokuda, "A widely tunable SOA-integrated DBR laser by combination of sampled and superstructure gratings," IEEE J. Lightwave Technol. **23**, 2331-2336 (2005).
13. F. A. Kish, D. Welch, R. Nagarajan, J. L. Pleumeekers, V. Lal, M. Ziari, A. Nilsson, M. Kato, S. Murthy, P. Evans, S. W. Corzine, M. Mitchell, P. Samra, M. Missey, S. DeMars, R. P. Schneider, M. S. Reffle, T. Butrie, J. T. Rahn, M. Van Leeuwen, J. W. Stewart, D. J. H. Lambert, R. C. Muthiah, H.-S. Tsai, J. S. Bostak, A. Dentai, K.-T. Wu, H. Sun, D. J. Pavinski, J. Zhang, J. Tang, J. McNicol, M. Kuntz, V. Dominic, B. D. Taylor, R. A. Salvatore, M. Fisher, A. Spannagel, E. Strzelecka, P. Studenkov, M. Raburn, W. Williams, D. Christini, K. J. Thomson, S. S. Agashe, R. Malendevich, G. Goldfarb, S. Melle, C. Joyner, M. Kaufman, and S. G. Grubb, "Current status of large-scale InP photonic integrated circuits," IEEE J. Sel. Top. Quantum Electron. **17**, 1470-1489 (2011).
14. B.-S. Kim, Y. Chung, and J.-S. Lee, "An efficient split-step time domain dynamic modeling of DFB/DBR laser diodes," IEEE J. Quantum Electron. **36**, 787-794 (2000).
15. Y. Chung, "Split-step time-domain modeling of dual-mode DFB laser diode for terahertz wave generation," Microw. Opt. Technol. Lett. **61**, 1895-1900 (2019).